Numerical method for dam break problem by using Godunov approach

M. F. Ahmad[a,c,*], M. Mamat[b,c], W. B. Wan Nik[a] and A. Kartono[c]

[a]*Department of Maritime Technology, Faculty of Maritime and Marine Sciences*
[b]*Department of Mathematics, Faculty of Sciences and Technology*
[c]*Physical Oceanography and Modeling Group, Institute of Oceanography and Environment,*
Universiti Malaysia Terengganu
21030 Kuala Terengganu, Terengganu, Malaysia

Abstract: *In this study a numerical scheme was developed in order to overcome the problem of shock wave for the test case of dam break. The numerical scheme was based on Godunov approach of finite volume method to solve the shallow water equation. In order to expedite and improve the solution an approximate Roe's Riemann solver associated with Monotone Upstream-centred Scheme for Conservation Laws (MUSCL) was applied. The results were presented in one and two dimensional and verifications were made with analytical solution. The results are comparable and a good agreement is achieved between numerical and analytical.*

Keywords: Godunov approach, Roe's scheme, Shallow water equation.

PACS: *47.11.Bc, 47.11.Df*

1   Introduction

A wide variety of physical phenomena are governed by mathematical models of the so-called shallow water type. An important class of problems of practical interest involves water flows with the free surface under the influence of gravity. This class includes tides in oceans, breaking of waves on shallow beaches, roll waves in open in channels, flood waves in rivers, surges and dam-break wave modeling. Shallow water equations have been widely used to model waves in the atmosphere, rivers, lakes and oceans as well as gravity waves in a smaller domain, e.g. surface waves in a bath. In order for shallow water equations to be valid, the wave length of the phenomenon they are supposed to model has to be much higher than the depth of the basin where the phenomenon takes place. Shallow water equations are especially suitable to model tides which have very large length scales (over hundreds of kilometer). For tidal motion, even a very deep ocean may be considered as shallow as its depth will always be much smaller than the tidal wave length [1].

_____

 * Corresponding Author: fadhli@umt.edu.my (M. F. Ahmad)

The most challenging feature of the shallow water wave equations is that they admit discontinuities and smooth solutions. Even the case in which the initial data is smooth can lead to discontinuous solutions in finite time. The non-linear character of the equations also means that analytical solutions to these equations are limited to only very special cases. Their non-linear character often yields discontinuous solutions. Such discontinuous often called 'shock' or 'shock waves', trigger the failure of a number of classical numerical methods. So, therefore the numerical methods are needed to approximate these equations. Their non-linear character often yields discontinuous solutions.

In order to overcome the discontinuities problem due to shock, many numerical schemes were developed. One of them is numerical scheme based on the Gudanov approach which is aiming the best solution around the discontinuities.

In this paper the explicit conservative schemes was examined for the solution of the one and two-dimensional homogeneous shallow water wave equations using the finite volume method associated with approximate Roe's Riemann solver. Then a well known analytical solution to the dam-break problem was used to assess the performance [2].

2   Shallow Water Equations

The two-dimensional shallow water equations with source terms may be written in vector form,

$$\frac{\partial U}{\partial t} + \frac{\partial F}{\partial x} + \frac{\partial G}{\partial y} = S \tag{1}$$

where U is the vector of conserved variables, F and G are the flux vectors in the x- and y-directions and S represents a source term vector. The vectors U, F and G can be expressed in terms of the primary variables u, v and h as

$$U = \begin{bmatrix} h \\ hu \\ hv \end{bmatrix}; \tag{2a}$$

$$F = \begin{bmatrix} hu \\ hu^2 + \frac{1}{2}gh^2 \\ huv \end{bmatrix}; \tag{2b}$$

$$G = \begin{bmatrix} hv \\ huv \\ hv^2 + \frac{1}{2}gh^2 \end{bmatrix}; \tag{2c}$$

$$S = \begin{bmatrix} 0 \\ gh(S_{0x} - S_{fx}) \\ gh(S_{0y} - S_{fy}) \end{bmatrix}; \tag{2d}$$

where g is the acceleration due to gravity, h the water depth, u and v are the flow velocity in the x- and y-directions, respectively. While S_{0x} and S_{0y} are the bed slopes in the two-Cartesian directions. The friction slopes S_{fx} and S_{fy} have been estimated using the Manning resistance law

$$S_{fx} = \frac{u\eta^2 \sqrt{u^2+v^2}}{h^{4/3}} \text{ and } S_{fy} = \frac{v\eta^2 \sqrt{u^2+v^2}}{h^{4/3}} \tag{3}$$

in which η is the Manning resistance coefficient. But in this paper, the bed was taken as constant in depth and friction was ignored, thus the source term is zero.

3   Numerical Method

There are a variety of numerical techniques for approximating, e.g. finite difference methods, finite element methods, finite volume methods, etc. In this paper, we will discuss the finite volume method associated with Roe's approximate Riemann solver [3, 4, 5]. Finite volume methods have several advantages over finite difference and finite element approaches. Finite volume methods combine the simplicity of finite difference methods with the geometric flexibility of finite element methods. Finite volume methods are based on the integral form of the conservation equations, thus a scheme in conservation form can easily be constructed to capture shock waves [6]. A finite difference scheme that is not conservative may propagate discontinuities at the wrong wave speed, if at all, giving inaccurate numerical results. Dissipation occurs when the travelling wave's amplitude decreases resulting in the numerical solution being smeared. Dispersion occurs when waves travel at different wave speeds and results in oscillations being present in the numerical results. Both dissipation and dispersion can cause very significant errors in the numerical results and sometimes give completely inaccurate numerical results [7].

3.1 Godunov approach of finite volume method

The aim of the Godunov approach is to provide the best solution around the discontinuity. Such discontinuities, often called 'shocks' or 'shock waves', trigger the failure of a number of finite different numerical methods. In these methods, space is discretised into volumes, more often called cells, hence the general term of finite volume method. The numerical solution is not characterised by its value at a set of points, but by its average over the cells. The evolution of the solution in a given cell is determined by the exchange (via fluxes) at the interfaces with all the neighbouring cells. In this approach, the fluxes are computed by solving Riemann problems at the interfaces between the cells.

The solution of the Riemann problem is a key ingredient of Godunov-type schemes. It is achieved using what is called a Riemann solver. In applying the finite volume scheme in this work, the Roe's Riemann solver was adopted to solve the Riemann problems. The Roe's solver [5, 8] may be the most widely applied Riemann solver to date. The basic idea of this solver is to change the hyperbolic system of conservation laws to be solved to an equivalent of linear systems.

3.2 MUSCL –type high-order method

In order to achieve high-order of accuracy and avoid spurious oscillation, an approach known as Monotone Upstream-centred Scheme for Conservation Laws (MUSCL) was adopted. This approach was first applied by Van Leer [9] in the first-order Godunov method. The approach involves

reconstructing the piece-wise constant $\{u_i^n, v_j^n\}$ by replacing with piecewise linear functions $u_i(x)$ and $v_j(y)$. As for the first order Godunov method, it could be assumed that u_i^n, v_j^n represents an integral average in cell $I_{i,j} = [x_{i-1/2}, x_{i+1/2}] \times [y_{j-1/2}, y_{j+1/2}]$.

A piece-wise linear, local reconstruction of u_i^n, v_j^n is given respectively

$$u_i(x) = u_i^n + \frac{(x - x_i)}{\Delta x} \Delta_i, \quad x \in [0, \Delta x] \tag{4a}$$

$$v_j(y) = v_j^n + \frac{(y - y_j)}{\Delta y} \Delta_j, \quad y \in [0, \Delta y] \tag{4b}$$

where $\Delta_i/\Delta x$ and $\Delta_j/\Delta y$ are a suitably chosen slope of $u_i(x)$ in cell I_i and $v_j(y)$ in cell I_j. The centre of the cell (x_i, y_j) in the local co-ordinates is $(x, y) = \left(\frac{1}{2}\Delta x, \frac{1}{2}\Delta y\right), u_i(x_i) = u_i^n$ and $v_j(y_j) = v_j^n$. The values of $u_i(x)$ and $v_j(y)$ at the extreme points play a fundamental role and are given respectively by

$$u_i^L = u_i(0) = u_i^n - \frac{1}{2}\Delta_i; \quad u_i^R = u_i(\Delta x) = u_i^n + \frac{1}{2}\Delta_i \tag{5a}$$

$$v_j^L = v_j(0) = v_j^n - \frac{1}{2}\Delta_j; \quad v_i^R = v_j(\Delta y) = v_j^n + \frac{1}{2}\Delta_j \tag{5b}$$

3.3 Slope limiter method

The construction of non-linear versions was taken by replacing the slopes $\Delta_{i,j}$ in the data reconstruction step with limited slope $\overline{\Delta}_{i,j}$. The limited slope is expressed in terms of slope limiter as

$$\overline{\Delta}_{i,j} = \Phi_{i,j}\Delta_{i,j} \tag{6}$$

where $\Delta_{i,j}$ is given by

$$\Delta_{i,j} = \frac{1}{2}(1 + \omega)\Delta u_{i-1/2, j-1/2} + \frac{1}{2}(1 - \omega)\Delta u_{i+1/2, j+1/2} \tag{7}$$

The $\omega = 1$ was used in the simulations. Combine the equation (6) and (7) gives

$$\begin{aligned}
u_i^L &= u_i(0) = u_i^n - \frac{1}{2}\Phi_i\Delta_{i-1/2}; \\
u_i^R &= u_i(\Delta x) = u_i^n + \frac{1}{2}\Phi_i\Delta_{i-1/2}
\end{aligned} \tag{8a}$$

$$v_j^L = v_j(0) = v_j^n - \frac{1}{2}\Phi_j \Delta_{j-1/2};$$

$$v_j^R = v_j(\Delta y) = v_j^n + \frac{1}{2}\Phi_j \Delta_{j-1/2}$$

(8b)

The slope limiters Φ_i and Φ_j proposed by Hirsch (1990) were used in the simulations. It is defined as

$$\Phi_i(r_x) = \max[0, \min(\beta r_x, 1), \min(r_x, \beta)],$$

(9a)

$$\Phi_j(r_y) = \max[0, \min(\beta r_y, 1), \min(r_y, \beta)],$$

(9b)

where the limiter parameter $1 \le \beta \le 2$, and the gradient ratio is given by

$$r_x = \begin{cases} \dfrac{u_{i+1} - u_i}{u_i - u_{i-1}}, & u_i - u_{i-1} \neq 0, \\ 0 & , u_i - u_{i-1} = 0 \end{cases}$$

(10a)

$$r_y = \begin{cases} \dfrac{v_{j+1} - v_j}{v_j - v_{j-1}}, & v_j - v_{j-1} \neq 0, \\ 0 & , v_j - v_{j-1} = 0 \end{cases}$$

(10b)

The choice β is 1.5 used in the slope limiter.

3.4 Eigenstucture in term of conserved variables

The Jacobian matrix (A) corresponding to the flux F' is given by

$$A = \begin{bmatrix} 0 & 1 & 0 \\ a^2 - \tilde{u}^2 & 2\tilde{u} & 0 \\ -\tilde{u}v & v & \tilde{u} \end{bmatrix}$$

(11)

The eigenvalues of A

$$\lambda_1 = \tilde{u} - a, \ \lambda_2 = \tilde{u}, \ \lambda_3 = \tilde{u} + a$$

(12)

The corresponding eigenvectors are

$$K^1 = \begin{bmatrix} 1 \\ \tilde{u} - a \\ \tilde{v} \end{bmatrix}, \ K^2 = \begin{bmatrix} 0 \\ 0 \\ 1 \end{bmatrix}, \ K^3 = \begin{bmatrix} 1 \\ \tilde{u} + a \\ \tilde{v} \end{bmatrix}$$

(13)

where

$$\tilde{u} = \frac{u^R \sqrt{h^R} + u^L \sqrt{h^L}}{\sqrt{h^R} + \sqrt{h^L}} \; ; \tag{14a}$$

$$\tilde{v} = \frac{v^R \sqrt{h^R} + v^L \sqrt{h^L}}{\sqrt{h^R} + \sqrt{h^L}} \; ; \tag{14b}$$

$$a = \sqrt{\frac{1}{2} g(h^R + h^L)} \; . \tag{14c}$$

where subscript R and L are the right and left states of variable, g = gravity acceleration.

The wave strengths $\tilde{\alpha}_1, \tilde{\alpha}_2, \tilde{\alpha}_3$ in term of the Roe averaged are:

$$\tilde{\alpha}_1 = \frac{\Delta u_1 (\tilde{u} + a) - \Delta u_2}{2a} \; ; \tag{15a}$$

$$\tilde{\alpha}_2 = \Delta u_3 - \tilde{v} \Delta u_1 \; ; \tag{15b}$$

$$\tilde{\alpha}_3 = \frac{-\Delta u_1 (\tilde{u} - a) + \Delta u_2}{2a} \tag{15c}$$

where

$$\Delta u_1 \equiv h_R - h_L \; ;$$

$$\Delta u_2 \equiv u_R h_R - u_L h_L \; \text{ or } \; q_R - q_L \; ;$$

$$\Delta u_3 \equiv h_R v_R - h_L v_L$$

Numerical flux has been described by Toro [10]

$$F_{i+\frac{1}{2}} = \frac{1}{2}(F_i^n + F_{i+1}^n) - \frac{1}{2} \sum_{i=1}^{m} \alpha_i |\lambda_i| K^i \tag{16}$$

From numerical flux above, the new value of the conserve variable can be determined with the equation

$$U_i^{n+1} = U_i^n - \frac{\Delta t}{\Delta x}\left[F_{i+1/2} - F_{i-1/2}\right] - \frac{\Delta t}{\Delta y}\left[G_{i+1/2} - G_{i-1/2}\right] \tag{17}$$

For the spatial step size, Δx, is fixed and we use a variable time step

$$\Delta t = \frac{C_{cfl} \Delta x}{\max_i \left(\left| \lambda_k \right| \right)} \tag{18}$$

where λ_k are the eigenvalues of the Jacobian matrix and C_{cfl} is the required CFL number (Courant, Friedrichs and Lewey). The scheme discussed in this paper is stable for $C_{cfl} \leq 1$. To ensure the error of a numerical scheme does not grow, the variables are non-dimensionalised so that the spatial and time step-sizes are less than one, i.e. $\Delta x < 1$ and $\Delta t < 1$ [11].

3.5 Boundary condition

The application of boundary conditions is fundamentally a physical problem. Numerically, we can implement the physically derived boundary conditions in such a way that the same scheme will be applicable to all cell i, $i = 1,\ldots,m$. Two fictitious cells are required next to each reflective or transmissive boundary condition. To simulate transmissive boundaries, we set

$$h_0^n = h_1^n, \qquad u_0^n = u_1^n, \tag{19a}$$

$$h_{m+1}^n = h_m^n, \quad u_{m+1}^n = u_m^n \tag{19b}$$

For the reflective boundaries are handled by the boundary conditions

$$h_0^n = h_1^n, \quad u_0^n = -u_1^n, \tag{20a}$$

$$h_{m+1}^n = h_m^n, \quad u_{m+1}^n = -u_m^n \tag{20b}$$

4   Verification of the Finite Volume Schemes

To determine the accuracy of the finite volume numerical scheme, we will test the case of one- and two-dimensional dam break problem.

4.1 Test case: the one-dimensional dam break problem

For analytical solution one-dimensional dam break problem has been tested by Stoker (1957). The test problem consists of 1D channel of length 1 m with walls at either end (Fig. 1). The initial velocity (u) is 0 and a barrier is present at $x = 0.5$, which is removed at $t = 0$ s. The initial conditions are

$$u(x,0) = 0 \text{ and } h(x) = \begin{cases} h_L & \text{if } 0 \leq x \leq 0.5 \\ h_R & \text{if } 0.5 < x \leq 1 \end{cases} \tag{21}$$

Stoker (1957) derived an analytical solution of the dam break problem which can be used to check the accuracy of the numerical schemes.

The analytical solution with $h_L = 1$ m and $h_R = 0.5$ m is illustrated in Figure 1 where the bore speed is approximately $S = 2.957918120187525$. For a more in depth analysis on how the value of S was obtained see [2] and [12].

Figures 2 and 3 show the comparison between analytical and numerical for water depth and water velocity at 0.04s respectively.
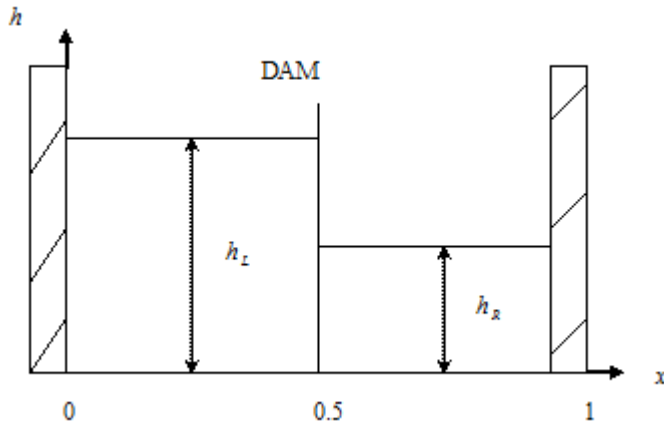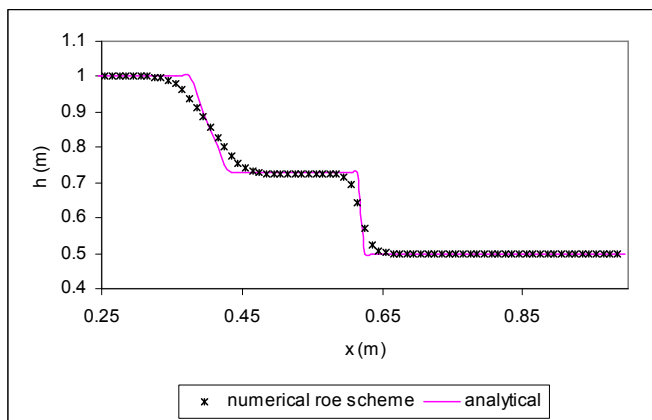

Figure 1: Initial conditions for the dam break problem.

Figure 2: Roe's numerical scheme and analytical solution of the dam break test problem for $t = 0.04$s.
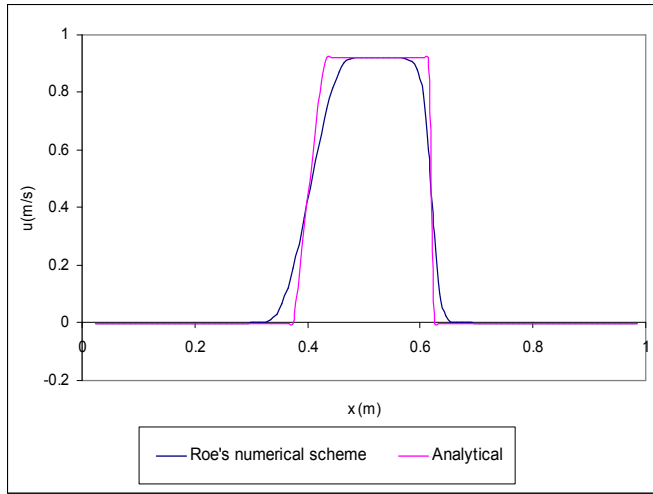
Figure 3: Roe's numerical scheme and analytical solution of the dam break test problem for $t = 0.04$s.

4.2 Test case: the two-dimensional dam break problem

For analytical solution two-dimensional dam break problem there is no reference. We use the case 1D dam break problem by stoker, but we made the case became two-dimensional with extend domain length along x- and y-directions. We assume the dam break on the whole. The test problem consists of 2D channel of length 1 m along x-direction and 1 m along y-direction. The initial velocities (u) and (v) are 0 m/s respectively for x- and y-directions and a barrier is present at $x = 0.5$ which is removed at $t = 0$ s the initial conditions are

$$u(x,0) = 0,$$
$$v(y,0) = 0 \text{ and}$$
$$h(x,y) = \begin{cases} h_{(x,y)L} & \text{if } 0 \le x \le 0.5 \\ h_{(x,y)R} & \text{if } 0.5 < x \le 1 \end{cases} \tag{22}$$

In this paper, we only tested the case at $t = 0.04$ s and $t = 0.08$ s. From the numerical result tested, it has represented the numerical scheme overall. For the initial condition, it shows in Figure 4.
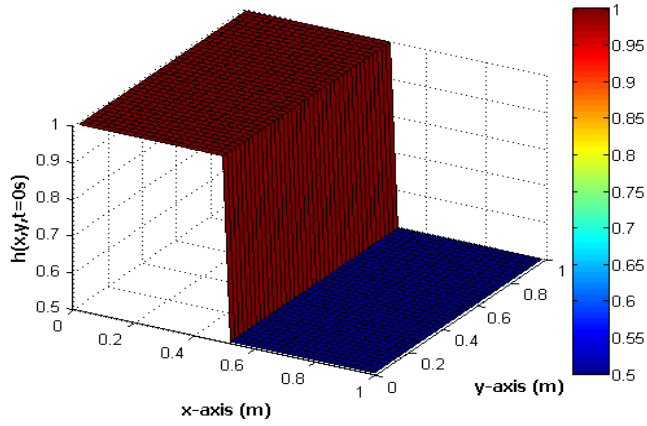
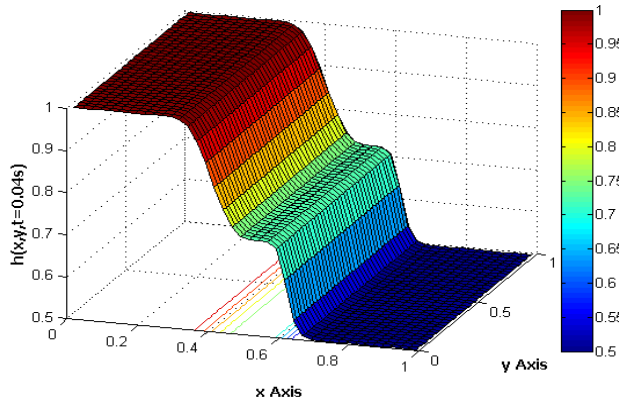Figure 4: Initial dam break problem.

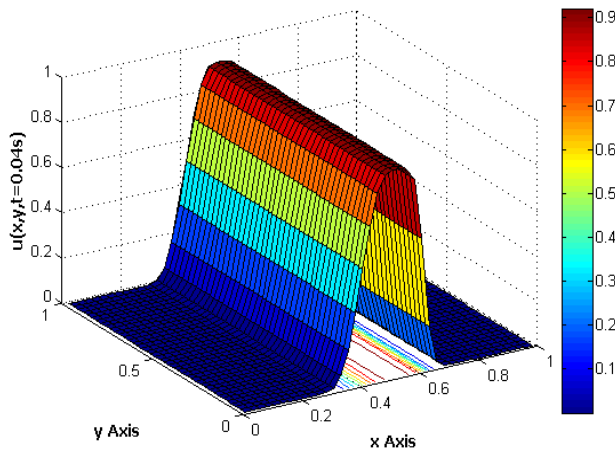Figure 5: Numerical result of Roe's scheme for dam break problem at $t = 0.04$ s in (h).

Figure 6: Numerical result of Roe's scheme for dam break problem along x-direction
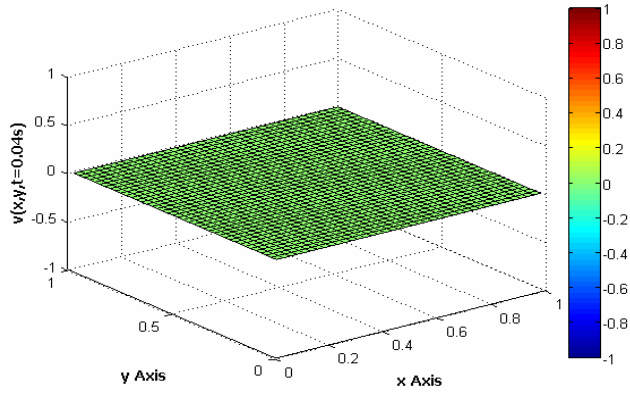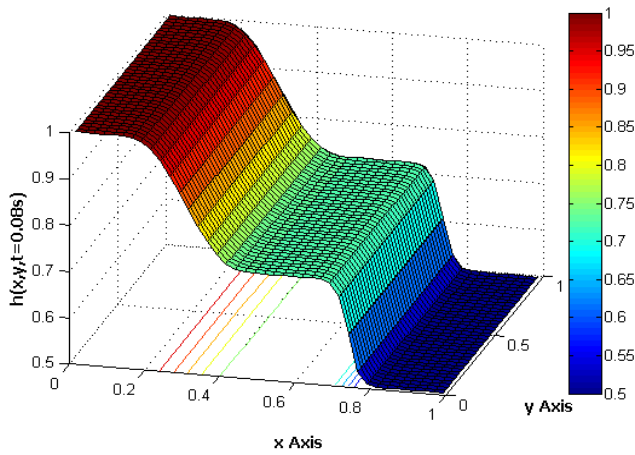at $t = 0.04$ s in (u).

Figure 7: Numerical result of Roe's scheme for dam break problem along *y*-direction
at *t* = 0.04 s in (*v*).

Figure 8: Numerical result of Roe's scheme for dam break problem at *t* =0.08 s in (*h*).
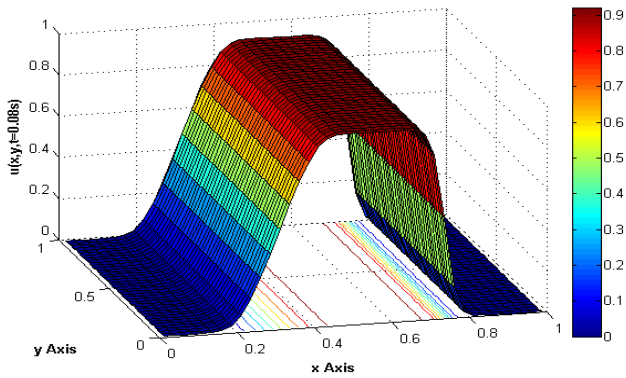

Figure 9: Numerical result of Roe's scheme for dam break problem along *x*-direction
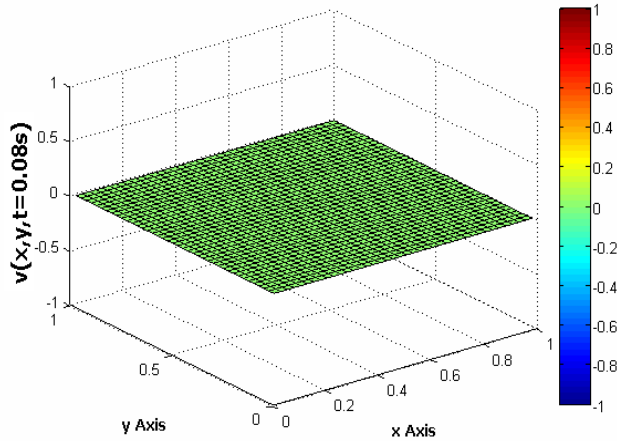at *t* = 0.08 s in (*u*).

Figure 10: Numerical result of Roe's scheme for dam break problem along *y*-direction
at *t* =0.08 s in (*v*).

Numerical results of two-dimensional dam break problem have been shown in Fig. 4 until Fig. 10. For Figures 5-7 show water depth (*h*), velocity in *x*-direction (*u*) and *y*-direction (*v*) respectively at *t* = 0.04 s. While Figures 8-10 show water depth (*h*), velocities in *x*-direction (*u*) and *y*-direction (*v*) respectively at *t* = 0.08 s. For the time steps, we used Courant Friedrichs-Lewy (CFL) number 0.9 and $\Delta x = 0.025$ m. We set transmissive boundary conditions along *x*- and *y*-directions.

5   Discussion and Conclusion

Finite volume method using Roe's approximate Riemann solver for the solution of the dam break problem in one and two dimensional has been described. The mathematical model used is represented by the two-dimensional shallow water equations. The advantages of using Riemann solvers to describe rapidly varying shallow water flows became apparent in the early 1990s. The shallow-water equations (SWEs) describe the conservation of mass and momentum in shallow water bodies, and are particularly amenable to solution by finite volume Godunov-type approaches where Roe's approximate Riemann solver can be used to evaluate in viscid fluxes.

The comparisons between analytical and numerical results for the 1D dam break problem have been shown, where the results could represent to two-dimensional in the same cases. Finite volume method provides more accurate results than Finite Difference Method [7].

Until recently it was considered that two-dimensional tools could not be applied to large domains, for reasons of computer time and memory. Further researches are desirable in order to solve some problem with source terms and also modified computing algorithm in order to obtain short time computing for the large domains.

From the numerical schemes and results discussed above, we can conclude that the Roe's scheme is very powerful to solve dam break problem in one- and two-dimensional. Sometimes Roe's scheme can produce the problems. But in general, Roe's scheme is quite stable and very non-viscous.

Acknowledgments

References

[1] E.F. Toro. *Shock Capturing Method for Free-Surface Shallow Flows*, John Wiley & Sons, Manchester, 2001.

[2] J.J. Stoker. *Water Waves*. Interscience, New York, NY, 1957.

[3] P. Glaister. *Difference Schemes for the Shallow Water Equations*, Numerical Analysis Report, Vol. 9/97, University of Reading, 1987.

[4] M.E. Hubbard and P. Garcia-Navarro. Flux Difference Splitting and the Balancing of Source Terms and Flux Gradients, *J. Comput. Phys.*, 165: 89-125, 2000.

[5] P.L. Roe. Approximate Riemann Solvers, Parameter Vectors and Difference Schemes, *J. Comput. Phys.*, 43: 357–372, 1981.

[6] M.F. Ahmad, M. Mamat, S. Rizki, I. Mohd and I. Abdullah, The Development of Numerical Method for Shock Waves and Wave Propagation on Irregular Bathymetry, *Applied Mathematical Science*, Vol. 5: 293-308, 2011.

[7] A. Valiani, V. Caleffi and A. Zanni. *Finite Volume Scheme for 2D Shallow-Water Equations Application to the Malpasset Dam-Break*, Università Degli Studi di Ferrara-Dipartimento di Ingegneria, 1999.

[8] P.L. Roe and J. Pike, *Efficient Construction and Utilization of Approximate Riemann Solutions, in Computing Methods in Applied Science and Engineering*, North-Holland, 1984.

[9] B. Van Leer, *Multidimensional Explicit Difference Schemes for Hyperbolic Conservation Laws, in Computing Methods in Applied Sciences and Engineering*, VI, Elsevier Science, Amsterdam, 1984.

[10] E.F. Toro, *Riemann Solvers and Numerical Methods for Fluid Dynamics*, Springer-Verlag, 1997.

[11] J. Hudson, *Numerical Techniques for Morphodynamic Modelling*, Doctoral Thesis, University of Reading, 2001.